

Dynamic and correlation properties of solid supported smectic-A filmsV. P. Romanov¹ and S. V. Ul'yanov²¹*Department of Physics, St. Petersburg State University, Petrodvorets, St. Petersburg 198504, Russia*²*Institute of Commerce and Economics, St. Petersburg 194018, Russia*

(Received 19 February 2002; revised manuscript received 27 September 2002; published 10 December 2002)

Dynamic properties and layer displacement–layer displacement correlation functions of the smectic-A films on a substrate are investigated. The eigenfrequencies spectrum and eigenmotions of the film are calculated within the framework of a discrete model. It was found that the static as well as dynamic properties of freely standing and solid supported smectic-A films differ significantly. In particular, the acoustic mode is absent in the films on a substrate and the surface tension is not essential for the film dynamics. The correlation length of the spatial layer displacement correlation functions is finite for films on a substrate in contrast to the free standing films. An effect of thermal fluctuations on the specular and diffuse x-ray scattering was analyzed.

DOI: 10.1103/PhysRevE.66.061701

PACS number(s): 61.30.Cz, 61.30.Eb, 83.80.Xz

I. INTRODUCTION

The smectic-A films have been intensively investigated during the past decade. The static and dynamic properties of the freely standing [1–14] and solid supported [15–19] films have been studied both theoretically and experimentally. So far the freely standing films have been studied in more detail. The spatial layer displacement–layer displacement correlation functions [2,5], eigenfrequencies and relaxation times of the film oscillations are analyzed [7,8,10,11,13]. The x-ray scattering from layered films is the basic experimental method of investigation of the static and dynamic film properties [1,2,4–9,12]. Information on the spatial correlations have been obtained from experiments on the specular and diffuse x-ray scattering in Refs. [1,4–6]. Recent experiments on the temporal correlation function of the x-ray scattering intensities [7,9,12] enable one to study the dynamic film properties.

Considerable attention has been drawn to the study of smectic-A films on a substrate [15–19]. Similar to the free standing films, the basic experimental method in this case is the x-ray scattering. This experiment yields information on the substrate roughness [19–21]. The correlation properties of solid supported films are studied in Ref. [19], where the layer displacements have been calculated for boundary conditions determined by the substrate roughness. In contrast to freely suspended films the layer displacement correlation function is caused by thermal fluctuations of layers as well as by replication of the substrate roughness. These contributions were supposed to be noncorrelated [19] and the results obtained for the free standing films [5] were used to determine the thermal fluctuations. Such an approach seems to be suitable for films with large elastic compression constant B when the thermal fluctuation contribution to the layer correlation function is small. In the general case this contribution may be of the same order as the input of the substrate roughness. As far as the quantitative information about substrate can be obtained from x-ray scattering experiments [19–21] it is necessary to describe the thermal layer fluctuation spectrum more accurately with the account for the boundary conditions on the solid surface.

In the present work we calculate the layer displacement

spatial correlation functions and eigenfrequencies of the smectic-A film on the plane substrate. It is shown that there exists no acoustic motion with the constant interlayer distances. The center of mass of the film motion is presented in all modes in contrast to optic oscillations in freely standing smectic-A films. We calculate dependencies of the eigenfrequencies and relaxation times on the in-plane component q_{\perp} of the wave vector within the framework of the discrete model [2,7,13]. Due to the presence of plane substrate the correlation lengths are finite contrary to the case of the freely standing films. In conclusion, we calculate the input of thermal fluctuations into intensities of the specular and the diffuse x-ray scattering.

The paper is organized as follows. In Sec. II we present the equations of motion for the film on substrate within the framework of the discrete model. The eigenfrequencies and relaxation times are also calculated. In Sec. III we obtain the spatial layer displacement–layer displacement correlation functions. Thick films are considered in Sec. IV. The contribution of the thermal fluctuations to the intensity of x-ray scattering is calculated in Sec. V.

II. BASIC EQUATIONS

Let us consider a smectic-A film located on the plane substrate. For z axis directed normally to the substrate the elastic part of the free energy can be written as

$$F = \frac{1}{2} \int_V d\mathbf{r} \left[B \left(\frac{\partial u}{\partial z} \right)^2 + K (\Delta_{\perp} u)^2 \right] + \frac{\gamma}{2} \int_S d\mathbf{r}_{\perp} |\nabla_{\perp} u|^2. \quad (2.1)$$

Here u is the displacement along the z axis, B and K are the layer compression and layer band elastic constants, respectively, γ is the surface tension. The first and the second terms in Eq. (2.1) describe the volume deformation and distortion of the free film surface, respectively.

We will analyze the dynamic and static films properties within the framework of the discrete model that has been successfully used in studying freely suspended films [2,7,13]. According to this model, equilibrium smectic layers

are flat with constant interlayer distances d . In a discrete model, Eq. (2.1) for N -layer film acquires the form

$$F = \frac{1}{2} \int_S d\mathbf{r}_\perp \left\{ \frac{B}{d} \left(\sum_{n=1}^{N-2} (u_{n+1} - u_n)^2 + u_{N-1}^2 \right) + dK \sum_{n=1}^{N-1} (\Delta_\perp u_n)^2 + \gamma (\nabla_\perp u_1)^2 \right\}. \quad (2.2)$$

Here we suppose that the N th layer is fixed by the substrate, $u_N = 0$, while the first layer refers to the free surface. Equations of layer motion are written within an assumption that the motion of the n th layer is caused by elastic and viscous forces, $-d^{-1}(\delta F/\delta u_n)$ and $\eta_3 \Delta_\perp (\partial u_n/\partial t)$, correspondingly, where η_3 is the layer sliding viscosity. The set of equations of motion in a linear approximation has the form [7,13]

$$\begin{aligned} \rho \frac{\partial^2 u_1(\mathbf{r}_\perp, t)}{\partial t^2} &= B \frac{u_2(\mathbf{r}_\perp, t) - u_1(\mathbf{r}_\perp, t)}{d^2} - K \Delta_\perp^2 u_1(\mathbf{r}_\perp, t) \\ &+ \frac{\gamma}{d} \Delta_\perp u_1(\mathbf{r}_\perp, t) + \eta_3 \Delta_\perp \frac{\partial u_1(\mathbf{r}_\perp, t)}{\partial t}, \\ \rho \frac{\partial^2 u_n(\mathbf{r}_\perp, t)}{\partial t^2} &= B \frac{u_{n+1}(\mathbf{r}_\perp, t) - 2u_n(\mathbf{r}_\perp, t) + u_{n-1}(\mathbf{r}_\perp, t)}{d^2} \\ &- K \Delta_\perp^2 u_n(\mathbf{r}_\perp, t) + \eta_3 \Delta_\perp \frac{\partial u_n(\mathbf{r}_\perp, t)}{\partial t}, \\ n &= 2, 3, \dots, N-1, \quad u_N(\mathbf{r}_\perp, t) = 0. \end{aligned} \quad (2.3)$$

Assuming that the film is infinite in the xy plane we can complete two-dimensional Fourier transformation. For the plane waves

$$u_n(\mathbf{q}_\perp, \omega) e^{i\mathbf{q}_\perp \cdot \mathbf{r}_\perp - i\omega t}$$

we obtain a set of linear homogeneous equations

$$\begin{aligned} \left(\rho \omega^2 + i\omega \eta_3 q_\perp^2 - \frac{B}{d^2} - K q_\perp^4 - \frac{\gamma}{d} q_\perp^2 \right) u_1 + \frac{B}{d^2} u_2 &= 0, \\ \left(\rho \omega^2 + i\omega \eta_3 q_\perp^2 - 2\frac{B}{d^2} - K q_\perp^4 \right) u_n + \frac{B}{d^2} u_{n-1} + \frac{B}{d^2} u_{n+1} &= 0, \\ n &= 2, 3, \dots, N-2, \\ \left(\rho \omega^2 + i\omega \eta_3 q_\perp^2 - 2\frac{B}{d^2} - K q_\perp^4 \right) u_{N-1} + \frac{B}{d^2} u_{N-2} &= 0. \end{aligned} \quad (2.4)$$

In Eq. (2.4) we omitted the arguments $(\mathbf{q}_\perp, \omega)$ in the amplitudes of Fourier harmonics u_n .

It is convenient to present these equations in the matrix form

$$\hat{A} \mathbf{u} = 0, \quad (2.5)$$

where the vector of layer displacements \mathbf{u} and tridiagonal matrix \hat{A} are [13]

$$\mathbf{u} = \begin{pmatrix} u_1 \\ u_2 \\ \vdots \\ u_{N-1} \end{pmatrix}, \quad \hat{A} = \begin{pmatrix} (2x+1-\alpha) & 1 & 0 & \cdots & 0 & 0 \\ 1 & 2x & 1 & \cdots & 0 & 0 \\ 0 & 1 & 2x & \cdots & 0 & 0 \\ \vdots & \vdots & \vdots & \ddots & \vdots & \vdots \\ 0 & 0 & 0 & \cdots & 2x & 1 \\ 0 & 0 & 0 & \cdots & 1 & 2x \end{pmatrix}. \quad (2.6)$$

Here we used the notations

$$\begin{aligned} x &= -1 + \frac{d^2}{2B} (\rho \omega^2 + i\omega \eta_3 q_\perp^2 - K q_\perp^4), \\ \alpha &= \frac{d\gamma q_\perp^2}{B}. \end{aligned} \quad (2.7)$$

Equation (2.5) has nonzero solution if its determinant is equal to zero,

$$\det \hat{A} = 0. \quad (2.8)$$

This equation may be presented in the form

$$U_{N-1}(x) + (1-\alpha)U_{N-2}(x) = 0, \quad (2.9)$$

where $U_n(x)$ is the Chebyshev polynomial of the second kind [22–24]. It can be written as a determinant of the tridiagonal matrix of the n th order,

$$U_n(x) = \begin{vmatrix} 2x & 1 & 0 & \cdots & 0 & 0 \\ 1 & 2x & 1 & \cdots & 0 & 0 \\ 0 & 1 & 2x & \cdots & 0 & 0 \\ \vdots & \vdots & \vdots & \ddots & \vdots & \vdots \\ 0 & 0 & 0 & \cdots & 2x & 1 \\ 0 & 0 & 0 & \cdots & 1 & 2x \end{vmatrix}. \quad (2.10)$$

Equation (2.9) has $N-1$ roots $x^{(l)}$, $l=1, 2, \dots, N-1$, which in general could be found numerically. For each root it is possible to get the pair of the system eigenfrequencies according to Eq. (2.7),

$$\omega_\pm^{(l)} = -i \frac{\eta_3 q_\perp^2}{2\rho} \pm \sqrt{\frac{2B}{\rho d^2} (1+x^{(l)}) + \frac{K q_\perp^4}{\rho} - \frac{\eta_3^2 q_\perp^4}{4\rho^2}}. \quad (2.11)$$

If α is equal to 0, 1, 2 or if $\alpha \rightarrow \infty$, Eq. (2.9) has an exact solution. For cases $\alpha \ll 1$ ($q_{\perp}^2 \ll B/\gamma d$) and $\alpha \gg 1$ ($q_{\perp}^2 \gg B/\gamma d$), which are important for the analysis, it is possible to find approximate solutions.

If in the case $q_{\perp}^2 \ll B/\gamma d$ we use the trigonometrical representation for Chebyshev polynomials [22–24],

$$U_n(\cos \theta) = \frac{\sin[(n+1)\theta]}{\sin \theta}, \quad (2.12)$$

then we get the following roots of the characteristic equation (2.9):

$$x^{(l)} = -\cos \frac{(2l-1)\pi}{2N-1} + \frac{2\alpha}{2N-1} \cos^2 \frac{(2l-1)\pi}{2(2N-1)},$$

$$l = 1, 2, \dots, N-1. \quad (2.13)$$

For $q_{\perp}^2 \gg B/\gamma d$ we get

$$x^{(l)} = -\cos \frac{l\pi}{N-1} - \frac{1}{\alpha(N-1)} \sin^2 \frac{l\pi}{N-1},$$

$$l = 1, 2, \dots, N-2, \quad x^{(N-1)} = \frac{\alpha}{2}. \quad (2.14)$$

For determination of the layer displacement amplitudes it is necessary to solve the set of homogeneous equations (2.5) for each eigenfrequency. For this purpose we present Eq. (2.5) in the form

$$\omega_{\pm}^{(l)} = -i \frac{\eta_3 q_{\perp}^2}{2\rho} \pm \sqrt{\frac{4B}{\rho d^2} \sin^2 \frac{(2l-1)\pi}{2(2N-1)} + \frac{4\gamma q_{\perp}^2}{(2N-1)\rho d} \cos^2 \frac{(2l-1)\pi}{2(2N-1)} + \frac{K q_{\perp}^4}{\rho} - \frac{\eta_3^2 q_{\perp}^4}{4\rho^2}}. \quad (2.19)$$

For typical values of the smectic-A material parameters: $B \sim 2.5 \times 10^7$ erg/cm³, $K \sim 10^{-6}$ dyn, $\gamma \sim 30$ erg/cm², $d \sim 30$ Å, $\eta_3 \sim 1$ Pz, $\rho \sim 1$ G/cm³, the inequality $K\rho/\eta_3^2 \ll 1$ is always fulfilled and hence we can neglect the contribution containing the elastic constant K . As it is seen from Eq. (2.19) the surface tension is more important for the first mode with $l=1$. In this case estimating $\sin[\pi/2(2N-1)]$ as $\pi/4N$ it is possible to present the expression for the radicand in Eq. (2.19) in the form

$$\frac{\pi^2 B}{4\rho L^2} + \frac{2\gamma q_{\perp}^2}{\rho L} - \frac{\eta_3^2 q_{\perp}^4}{4\rho^2}, \quad (2.20)$$

where $L=Nd$ is the film thickness. If the term with the surface tension were the principal one, the following relation is to be fulfilled:

$$\begin{pmatrix} u_2 \\ u_3 \\ u_4 \\ \vdots \\ u_{N-1} \\ 0 \end{pmatrix} = -2x^{(l)} \begin{pmatrix} u_1 \\ u_2 \\ u_3 \\ \vdots \\ u_{N-2} \\ u_{N-1} \end{pmatrix} - \begin{pmatrix} u_1 \\ u_1 \\ u_2 \\ \vdots \\ u_{N-3} \\ u_{N-2} \end{pmatrix} + \alpha \begin{pmatrix} u_1 \\ 0 \\ 0 \\ \vdots \\ 0 \\ 0 \end{pmatrix}. \quad (2.15)$$

Using Eq. (2.15), we can express the amplitudes of layer displacements through the amplitude of the first layer, which can be chosen arbitrary. Taking into account the recursion relation between Chebyshev polynomials [22–24]

$$U_n(x) - 2xU_{n-1}(x) + U_{n-2}(x) = 0, \quad (2.16)$$

and supposing formally that

$$U_0(x) = 1, \quad U_{-1}(x) = 0, \quad (2.17)$$

we get from Eq. (2.15),

$$u_n^{(l)} = (-1)^{n-1} [U_{n-1}(x^{(l)}) + (1-\alpha)U_{n-2}(x^{(l)})],$$

$$n, l = 1, 2, \dots, N-1. \quad (2.18)$$

The amplitude of the first layer is assumed to be equal to unity for each mode.

Now let us compare the dynamic properties of solid supported and freely standing smectic-A films. First of all the role of surface tension essentially differs in these systems. In freely standing films, the surface tension forces produce the acoustic mode having the largest relaxation time or the lowest frequency [13]. In contrast to this case, in the solid supported film dynamics the surface tension γ does not noticeably affect the spectrum of eigenfrequencies. Indeed, as it follows from Eq. (2.13), Eq. (2.11) may be written as

$$1 < \frac{8\gamma L}{\pi^2 B} q_{\perp}^2 < \left(\frac{8\gamma}{\pi\eta_3} \right)^2 \frac{\rho}{B}. \quad (2.21)$$

These inequalities cannot be valid simultaneously since in smectic A the following relation between material constants is always valid:

$$\frac{8\gamma}{\pi\eta_3} \sqrt{\frac{\rho}{B}} < 1. \quad (2.22)$$

Therefore, the dynamics of a solid supported film of any thickness is determined by elastic and viscous bulk properties.

Figure 1 shows the displacements of the five-layer smectic-A film on a plane substrate for all four modes. Con-

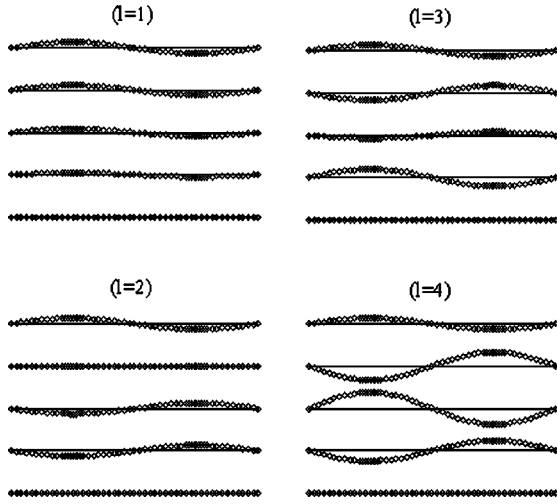


FIG. 1. Types of eigenmodes for the five-layer smectic-A film on a substrate.

trary to the freely standing films in this system the acoustic mode keeping the interlayer distances is absent. At the same time there are no purely optic oscillations with fixed position of the center of mass. In Figs. 2 and 3 the dependencies of

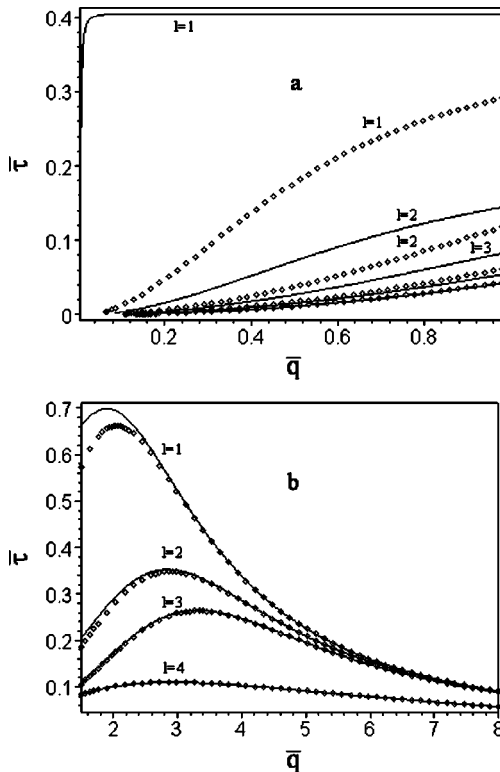


FIG. 2. Dependences of relaxation times $\tau_+^{(l)}$ on the wave number for five-layer smectic-A films. The dimensionless time $\bar{\tau} = \tau\sqrt{KB}/\eta_3 d$ and dimensionless wave number $\bar{q} = q_\perp \sqrt{d\gamma}/B$ are used. Diamonds correspond to the solid supported film and solid lines correspond to the freely standing film. The mode numbers are numerated from top to bottom. The relaxation times for the solid supported film are calculated by (a) Eqs. (2.13), (2.11), and (2.23); (b) Eqs. (2.14), (2.11), and (2.23).

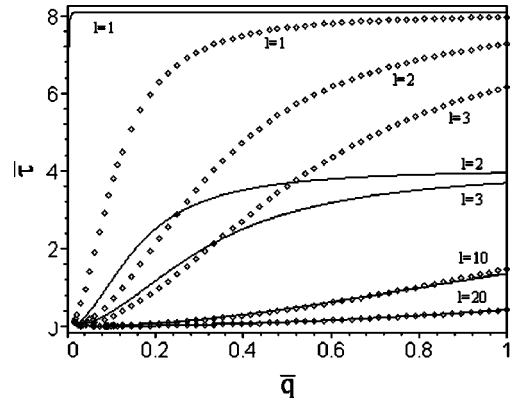


FIG. 3. Dependences of relaxation times $\tau_+^{(l)}$ on the wave number for 100-layer smectic-A films. The dimensionless variables and styles of lines are the same as in Fig. 2. The curves from top to bottom relate to $l=1,2,3,10,20$, respectively.

relaxation times

$$\tau_+^{(l)} = -\frac{i}{\omega_+^{(l)}}, \quad l=1,2,\dots,N-1, \quad (2.23)$$

on wave number q_\perp are presented. The calculations were carried out for films containing five and 100 layers. The results of calculations for the freely standing films with the same parameters are shown in these figures for comparison. It is seen that the relaxation times of the first mode for solid supported and freely standing films approach each other with increasing q_\perp value. The difference between relaxation times for these two cases disappears for modes with large mode numbers l .

III. LAYER DISPLACEMENT FLUCTUATIONS

In order to obtain the spatial correlation functions of the layer displacements we use the expression (2.2) for the free energy. In Fourier representation it can be written as

$$F = \frac{1}{2} \int \frac{d\mathbf{q}_\perp}{(2\pi)^2} \sum_{n,m=1}^{N-1} u_n(\mathbf{q}_\perp) M_{nm} u_m(-\mathbf{q}_\perp), \quad (3.1)$$

where the symmetric tridiagonal matrix \hat{M} of the $N-1$ order has the form

$$\hat{M} = -\frac{B}{d} \begin{pmatrix} (2y+1-\alpha) & 1 & 0 & \cdots & 0 & 0 \\ 1 & 2y & 1 & \cdots & 0 & 0 \\ 0 & 1 & 2y & \cdots & 0 & 0 \\ \vdots & \vdots & \vdots & \ddots & \vdots & \vdots \\ 0 & 0 & 0 & \cdots & 2y & 1 \\ 0 & 0 & 0 & \cdots & 1 & 2y \end{pmatrix}. \quad (3.2)$$

Here we used the notation

$$y = -1 - \frac{d^2 K q_{\perp}^4}{2B}. \quad (3.3)$$

The spatial layer displacement–layer displacement correlation function is equal to

$$\langle u_n(\mathbf{r}_{\perp}) u_m(\mathbf{0}) \rangle = \frac{k_B T}{(2\pi)^2} \int d\mathbf{q}_{\perp} (\hat{M}^{-1})_{nm} e^{i\mathbf{q}_{\perp} \cdot \mathbf{r}_{\perp}}, \quad (3.4)$$

where k_B is the Boltzmann constant and T is the temperature. The inverse matrix elements $(\hat{M}^{-1})_{nm}$ can be obtained by using the cofactors M_{nm} of the matrix \hat{M} elements. Using Eq. (2.10) for the Chebyshev polynomials we obtain the expressions for the elements of the first row and first column of matrix \hat{M} ,

$$M_{1n} = M_{n1} = (-1)^{n+1} U_{N-n-1}(y), \quad n = 1, 2, \dots, N-1. \quad (3.5)$$

The cofactors of the remaining elements can be expressed as

$$M_{nm} = (-1)^{n+m} [U_{m-1}(y) + (1-\alpha)U_{m-2}(y)] U_{N-n-1}(y), \quad n \geq m > 1. \quad (3.6)$$

Using the expression of the matrix \hat{M} determinant,

$$\det \hat{M} = U_{N-1}(y) + (1-\alpha)U_{N-2}(y), \quad (3.7)$$

and Eq. (2.17) we obtain the elements of the inverse matrix in the form

$$\begin{aligned} (\hat{M}^{-1})_{nm} &= (-1)^{n+m+1} \frac{d}{B} \\ &\times \frac{[U_{m-1}(y) + (1-\alpha)U_{m-2}(y)] U_{N-n-1}(y)}{U_{N-1}(y) + (1-\alpha)U_{N-2}(y)}, \\ n \geq m, \quad n, m &= 1, 2, \dots, N-1, \end{aligned} \quad (3.8)$$

$$(\hat{M}^{-1})_{nm} = (\hat{M}^{-1})_{mn}.$$

The spatial layer displacement correlation functions in a solid supported smectic-A film can be calculated by using Eqs. (3.4) and (3.8). Integrating over the angle in Eq. (3.4) we obtain

$$\langle u_n(\mathbf{r}_{\perp}) u_m(\mathbf{0}) \rangle = \frac{k_B T}{2\pi} \int d q_{\perp} q_{\perp} J_0(q_{\perp} r_{\perp}) (\hat{M}^{-1})_{nm}(q_{\perp}), \quad (3.9)$$

where $J_0(x)$ is the zeroth-order Bessel function.

The results of numerical calculations of the layer displacement correlation functions obtained from Eqs. (3.8) and (3.9) are shown in Figs. 4–7. The dependencies of correlation functions $\langle u_n(0) u_m(0) \rangle$ on the layer indices are presented in Fig. 4. It is seen that the correlation functions of the films on a substrate differ noticeably from the free standing films. In particular, the correlation functions are not symmetric with respect to the center of the film as it is shown in Fig.

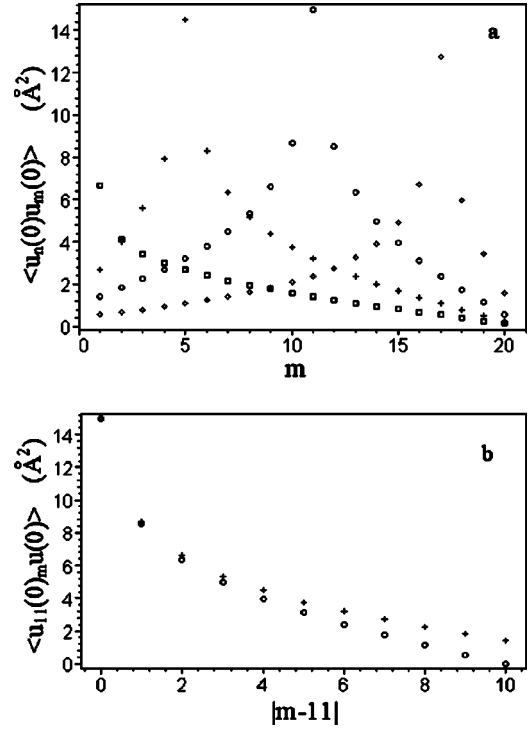


FIG. 4. The dependence of the correlation function $\langle u_n(0) u_m(0) \rangle$ on the layer number m for fixed n in a 21-layer film with a fixed 21st layer. (a) Squares, $n=1$; crosses, $n=5$; circles, $n=11$; and diamonds, $n=17$. (b) The dependence of the correlation function $\langle u_n(0) u_m(0) \rangle$ for $n=11$ on the layer indexes difference $|m-11|$. Crosses and circles correspond to approaching a free surface and a substrate, respectively.

4(b). The mean square fluctuations for films of various thickness are shown in Fig. 5. The dependencies of correlation functions $\langle u_n(r_{\perp}) u_m(0) \rangle$ on the in-plane distance r_{\perp} for 11-layer film are presented in Fig. 6. It is shown that for the solid supported films with infinite surface the correlation length is finite contrary to the freely standing films. Note that the correlation length decreases on approaching the solid surface. Formally the finite value of the correlation length results from the absence of singularities at the lower and upper

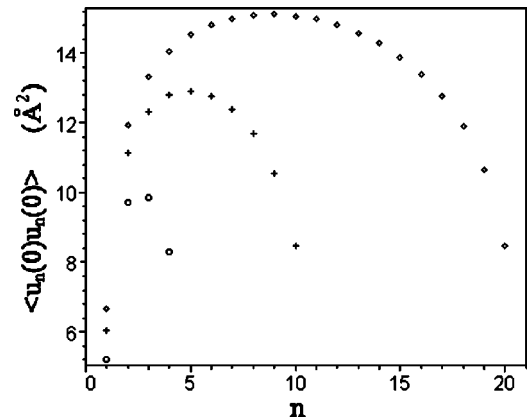


FIG. 5. Thermal layer fluctuations in N -layer smectic-A films with a fixed N th layer and the free first layer. For circles $N=5$, for crosses $N=11$, and for diamonds $N=21$.

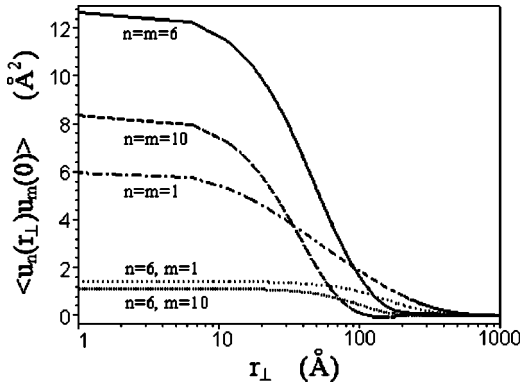


FIG. 6. The dependence of the spatial correlation function $\langle u_n(r_\perp)u_m(0) \rangle$ on the in-plane distance r_\perp for the 11-layer smectic-A film on a substrate. The free surface refers to the first layer.

limits of integration in Eq. (3.9). The inverse matrix elements for the solid supported film are finite for the zero wave number $q_\perp = 0$,

$$(\hat{M}^{-1})_{nm}(0) = \frac{d}{B}(N-n), \quad n \geq m, \quad n, m = 1, 2, \dots, N-1, \quad (3.10)$$

$$(\hat{M}^{-1})_{nm} = (\hat{M}^{-1})_{mn}.$$

In Eq. (3.9) the integrand decreases rapidly with increasing wave number q_\perp . Hence, we can expect that the main input

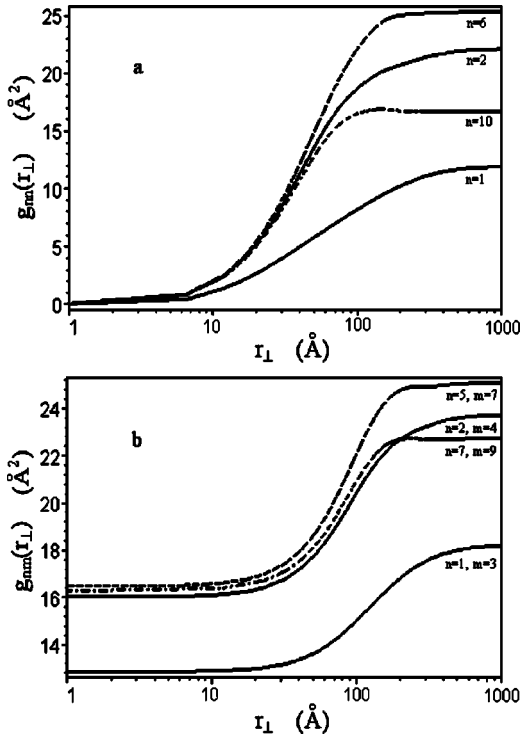


FIG. 7. The dependence of the height difference correlation function $g_{nm}(r_\perp)$ on the in-plane distance r_\perp for the 11-layer smectic-A film on a substrate: (a) $n = m$, (b) $n \neq m$. The free surface refers to the first layer.

to the integral in Eq. (3.9) is formed in the region that can be obtained from Eq. (3.3), i.e., $q_\perp \leq q_M$, where $q_M = (2B/Kd^2)^{1/4}$. This value of the wave number corresponds to the characteristic length $r_c = (Kd^2/2B)^{1/4} \sim 20 \text{ \AA}$, this value being in accordance with the results of numerical calculations presented in Fig. 6. In the freely standing films for small wave numbers, $q_\perp \rightarrow 0$, the inverse matrix elements have the singularity $(\hat{M}^{-1})_{nm}(q_\perp) \sim 1/\gamma q_\perp^2$, which results in the logarithmic divergence at the lower integration limit in Eq. (3.9). Figure 7 shows the height difference correlation function $g_{nm}(r_\perp)$, where

$$g_{nm}(r_\perp) = \langle [u_n(r_\perp) - u_m(0)]^2 \rangle. \quad (3.11)$$

It is seen from the figures that for small r_\perp functions $g_{nm}(r_\perp)$ with equal difference $|n-m|$ coincide, excluding cases when one of the layers is the film boundary.

It is interesting to analyze the correlation function $\langle u_n(r_\perp)u_m(0) \rangle$ behavior in limiting cases $r_\perp \rightarrow 0$ and $r_\perp \rightarrow \infty$. If we expand the Bessel function $J_0(q_\perp r_\perp)$, Eq. (3.9), in power series for $r_\perp \rightarrow 0$ we find that the correlation function decreases with decreasing distance as

$$\langle u_n(r_\perp)u_m(0) \rangle = \langle u_n(0)u_m(0) \rangle - A_{nm}r_\perp^2, \quad (3.12)$$

where A_{nm} is positive coefficient. For analyses of the correlation function $\langle u_n(r_\perp)u_m(0) \rangle$ behavior at a large distances it is convenient to use the asymptotic expansion of the Bessel function [27],

$$\int_0^{+\infty} q dq J_0(qr) f(q) \sim r^{-2} \sum_{k=0}^{\infty} c_k r^{-k} \quad (r \rightarrow \infty), \quad (3.13)$$

where

$$c_k = \frac{2^{k+1} \Gamma\left(\frac{k}{2} + 1\right)}{k! \Gamma\left(-\frac{k}{2}\right)} f^{(k)}(0), \quad (3.14)$$

$\Gamma(x)$ is the gamma function, and $f(q)$ is a regular function for $q > 0$ and it decreases for $q \rightarrow +\infty$. Substituting the expansion (3.13) into Eq. (3.9) we find that all coefficients of the asymptotic expansion are equal to zero, $c_k = 0$. Indeed for $k = 2l$ we get $1/\Gamma(-l) = 0$ and for $k = 2l + 1$ all derivatives of the function $f(q)$ at $q_\perp = 0$ are equal to zero, $f^{(2l+1)}(0) = 0$. Thus at large distances, $r_\perp \rightarrow \infty$, the correlation function decreases faster than according to power law.

IV. THICK FILMS

Let us compare the results obtained for the solid supported films with the correlation function of infinite Smectic A calculated within the framework of the continual model [25]. In this model all characteristic lengths are supposed to be much larger in comparison to the interlayer distance d . The layer displacement correlation function in \mathbf{q} representation is equal to [26]

$$\langle |u(\mathbf{q})|^2 \rangle = \frac{k_B T}{Bq_z^2 + Kq_\perp^4}. \quad (4.1)$$

For comparison it is convenient to use (\mathbf{q}_\perp, z) representation. Using Eq. (4.1) we get

$$\begin{aligned} \langle u(z, \mathbf{q}_\perp) u(z', -\mathbf{q}_\perp) \rangle &= \frac{1}{2\pi} \int_{-\infty}^{+\infty} dq_z e^{iq_z(z-z')} \frac{k_B T}{Bq_z^2 + Kq_\perp^4} \\ &= \frac{k_B T}{2B\lambda q_\perp^2} e^{-|z-z'|\lambda q_\perp^2}, \end{aligned} \quad (4.2)$$

where $\lambda = \sqrt{K/B}$. According to Eq. (3.1) the correlation function in the discrete model is equal to

$$\langle u_n(\mathbf{q}_\perp) u_m(-\mathbf{q}_\perp) \rangle = k_B T (\hat{M}^{-1})_{nm}. \quad (4.3)$$

In thick films number of layers is large, $N \gg 1$. We shall consider the inner layers n and m determined by the conditions $1 \ll n, m \ll N$. For comparison with the continual model we also suppose that

$$q_\perp^{-1} \gg \sqrt{d\lambda}. \quad (4.4)$$

In this case Eqs. (3.8) and (4.3) can be significantly simplified. Note that the argument of the Chebyshev polynomial, y , determined by Eq. (3.3) is negative and $y \leq -1$. Hence, it is convenient to express the Chebyshev polynomials $U_n(y)$ through the hyperbolic functions [24],

$$U_n(-\cosh \theta) = (-1)^n \frac{\sinh(n+1)\theta}{\sinh \theta}, \quad (4.5)$$

where

$$\cosh \theta = -y = 1 + \frac{d^2 K q_\perp^4}{2B}. \quad (4.6)$$

From Eqs. (4.4) and (4.6) we have

$$\theta \approx d\lambda q_\perp^2. \quad (4.7)$$

In this case for Chebyshev polynomials $U_n(y)$ of the higher orders, $n \gg 1$, we get an approximate relation

$$U_n(-\cosh \theta) \approx (-1)^n \frac{e^{(n+1)\theta}}{2\theta}. \quad (4.8)$$

Substituting this expression into Eqs. (3.8) and (4.3) we get

$$\langle u_n(\mathbf{q}_\perp) u_m(-\mathbf{q}_\perp) \rangle = \frac{k_B T}{2B\lambda q_\perp^2} e^{-|n-m|d\lambda q_\perp^2}. \quad (4.9)$$

Using the notations $nd=z$ and $md=z'$ we obtain the continual model expression, Eq. (4.2). So for thick films the results in the discrete and in the continual [25] models coincide. The same is valid for the free standing films.

V. X-RAY SCATTERING

The obtained results for the layer displacement correlation functions can be used for calculation of the intensity of x-ray scattering from the solid supported smectic-A films. The x-ray scattering intensity $I(\mathbf{q})$ is determined by the correlation function of the electron densities,

$$I(\mathbf{q}) \sim \langle \rho(\mathbf{q}) \rho(-\mathbf{q}) \rangle, \quad (5.1)$$

where $\rho(\mathbf{q})$ is the Fourier transformation of the electron density, \mathbf{q} is the scattering vector. In Gaussian approximation the correlation function of the electron densities, $\langle \rho(\mathbf{q}) \rho(-\mathbf{q}) \rangle$, has the form [1,5,7,14]

$$\begin{aligned} \langle \rho(\mathbf{q}) \rho(-\mathbf{q}) \rangle &= 2\pi \rho_s^2 |\rho_M(q_z)|^2 \sum_{n,m=1}^N \exp[-iq_z(n-m)d] \\ &\quad \times \int_0^\Lambda r_\perp dr_\perp J_0(q_\perp r_\perp) \exp\left[-\frac{q_z^2}{2} g_{nm}(r_\perp)\right] \\ &= 2\pi \rho_s^2 |\rho_M(q_z)|^2 \sum_{n,m=1}^N \exp[-iq_z(n-m)d] \\ &\quad \times \exp\left[-\frac{q_z^2}{2} [\langle u_n^2(\mathbf{r}_\perp=0) \rangle + \langle u_m^2(\mathbf{r}_\perp=0) \rangle]\right] \\ &\quad \times G_{nm}(q_\perp, q_z), \end{aligned} \quad (5.2)$$

where

$$G_{nm}(q_\perp, q_z) = \int_0^\Lambda r_\perp dr_\perp J_0(q_\perp r_\perp) \exp[q_z^2 \langle u_n(\mathbf{r}_\perp) u_m(0) \rangle]. \quad (5.3)$$

Here ρ_s is the surface density of molecules in the smectic layer, $\rho_M(q_z)$ is the Fourier transformation of the linear electron density in the molecule along the z axis, Λ is the linear size of the film surface. The scattering vector has the components $\mathbf{q} = (\mathbf{q}_\perp, q_z)$.

The intensity of the specular x-ray scattering is determined by Eqs. (5.2) and (5.3) with $\mathbf{q}_\perp = 0$. The results of calculations for the film containing five layers are shown in Fig. 8. The material parameters of smectic A are the same as in the previous sections. In these calculations we neglect the molecular form-factor dependence on the wave number q_z , $\rho_M(q_z) = \rho_M^0$. It should be noted that the intensity of the specular x-ray scattering tends to the constant value $\pi \rho_s^2 |\rho_M^0|^2 \Lambda^2$ with increasing wave number q_z . This effect is caused by the specular reflection from the plane boundary layer $u_N = 0$. Such behavior of the specular x-ray scattering from the solid supported smectic-A films differs significantly from that for the freely standing films [1,5,6]. As it is seen from Eqs. (5.2) and (5.3) the intensity of the specular x-ray scattering from the freely standing films tends to zero with increasing q_z [5].

For calculation of the diffuse x-ray scattering from the smectic-A film on a substrate we can fix the component q_z of the scattering vector and vary the in-plane component q_\perp only. In the integral $G_{nm}(q_\perp, q_z)$ entering Eq. (5.2) we ex-

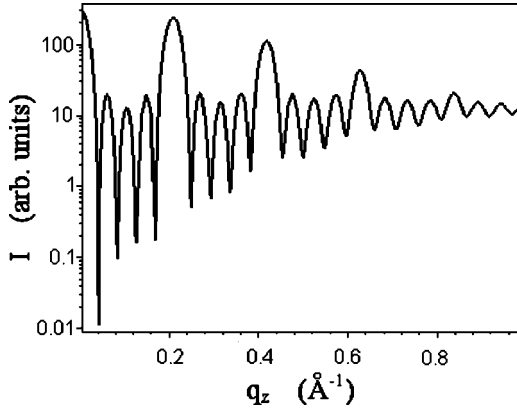


FIG. 8. The calculated dependence of the intensity of the specular x-ray scattering from the five-layer solid supported smectic-A film on the wave number q_z .

pand the exponential function into series keeping the first two terms only. This approximation is valid for moderate values of the wave number q_z . Usually the experiments on the diffuse x-ray scattering are performed in the vicinity of the first Bragg's peak, $q_z = 2\pi/d \sim 2 \times 10^7 \text{ cm}^{-1}$. In the smectic-A film on a substrate the correlation function $\langle u_n(r_\perp)u_m(0) \rangle$ attains the maximum value $\sim 10 \text{ \AA}^2$ at $r_\perp = 0$. Therefore, the exponent $q_z^2 \langle u_n(r_\perp)u_m(0) \rangle$ is of the order of 0.4 and decreases rapidly with increase of the in-plane distance r_\perp . At the same time according to Eq. (5.3) the region $r_\perp \sim 0$ enters the integral with the zero weight.

As long as the in-plane film size obeys the inequality $\Lambda \gg r_c$ the upper integration limit in Eq. (5.3) can be extended to infinity. For $q_\perp \neq 0$ integral (5.3) can be presented in the form

$$G_{nm}(q_\perp, q_z) \approx q_z^2 \int_0^\infty r_\perp dr_\perp J_0(q_\perp r_\perp) \langle u_n(\mathbf{r}_\perp) u_m(0) \rangle, \quad (5.4)$$

where the correlation function $\langle u_n(\mathbf{r}_\perp) u_m(0) \rangle$ is determined by Eq. (3.9). Using the relation

$$\int_0^\infty r dr J_0(qr) J_0(q'r) = \frac{1}{q} \delta(q' - q), \quad (5.5)$$

where $\delta(x)$ is the δ function, we get

$$G_{nm}(q_\perp, q_z) \approx \frac{k_B T q_z^2}{2\pi} (\hat{M}^{-1})_{nm}(q_\perp). \quad (5.6)$$

The results of the diffuse x-ray scattering calculations are shown in Fig. 9. The scattered intensity is constant up to the values $q_\perp \sim 10^5 \text{ cm}^{-1}$ and decreases in the region of characteristic wave number $q_M \sim 2 \times 10^6 \text{ cm}^{-1}$, this value is in accordance with the correlation length r_c . According to Eq. (5.6) the decrease of the diffuse x-ray scattering is determined by the matrix \hat{M}^{-1} . In the thick films for moderate wave numbers, $q_\perp < 1/\sqrt{d\lambda}$, the elements of \hat{M}^{-1} matrix have the form according to Eq. (4.9),

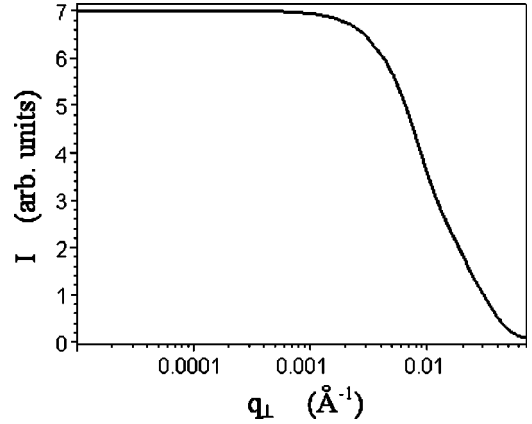


FIG. 9. The calculated dependence of diffuse x-ray scattering intensity on q_\perp near the first Bragg's peak $q_z = 0.21 \text{ \AA}^{-1}$ for the solid supported five-layer smectic-A film.

$$(\hat{M}^{-1})_{nm}(q_\perp) \approx \frac{e^{-|n-m|d\lambda q_\perp^2}}{2B\lambda q_\perp^2}. \quad (5.7)$$

For very large wave numbers, $q_\perp \gg 1/\sqrt{d\lambda}$, the elements of \hat{M}^{-1} matrix decay with increasing q_\perp as

$$(\hat{M}^{-1})_{nm}(q_\perp) \sim \frac{d}{B(\sqrt{d\lambda} q_\perp)^{4+4|n-m|}} \quad (q_\perp \rightarrow \infty). \quad (5.8)$$

Note that this region of the wave numbers is not studied experimentally [19,21]. So the decrease of the diffuse x-ray scattering intensity is not described by the universal power law. At the same time in some regions of q_\perp the damping can be approximated by the law $q_\perp^{-\gamma}$, where the value of γ is within the limits $2 \leq \gamma \leq 4$ in accordance with Eqs. (5.8), and (5.7).

In x-ray scattering studies of solid supported smectic-A films, the roughness of substrate attracts considerable interest [15–19]. Usually, the correlation length of the substrate inhomogeneity is of the order of $5 \times 10^2 \text{ \AA}$ [16,17], i.e., sufficiently larger than the correlation length of the layer thermal fluctuations in this system. Thus the decreasing of x-ray scattering caused by the roughness replication and thermal fluctuations of layers occurs in different regions of the wave number q_\perp values. It should be noted that this difference increases in films with larger values of the elastic constant $B \sim 10^9 - 10^{10} \text{ erg/cm}^3$. Such films have been widely used in the experiments [15–19].

In order to study the dynamic properties of solid supported films it should be desirable to measure the x-ray scattering intensities temporal correlation functions similar to experiments for the freely standing smectic-A films [7,9,12].

ACKNOWLEDGMENT

This work was supported by the RFBR Grant No. 02-02-16577.

- [1] D.J. Tweet, R. Holyst, B.D. Swanson, H. Stragier, and L.B. Sorensen, *Phys. Rev. Lett.* **65**, 2157 (1990).
- [2] R. Holyst, *Phys. Rev. A* **44**, 3692 (1991).
- [3] A.N. Shalaginov and V.P. Romanov, *Phys. Rev. E* **48**, 1073 (1993).
- [4] J.D. Shindler, E.A.L. Mol, A. Shalaginov, and W.H. de Jeu, *Phys. Rev. Lett.* **74**, 722 (1995).
- [5] E.A.L. Mol, J.D. Shindler, A.N. Shalaginov, and W.H. de Jeu, *Phys. Rev. E* **54**, 536 (1996).
- [6] E.A.L. Mol, G.C.L. Wong, J.M. Petit, F. Rieutord, and W.H. de Jeu, *Phys. Rev. Lett.* **79**, 3439 (1997).
- [7] A. Poniewierski, R. Holyst, A.C. Price, L.B. Sorensen, S.D. Kevan, and J. Toner, *Phys. Rev. E* **58**, 2027 (1998).
- [8] A. Poniewierski, R. Holyst, A.C. Price, and L.B. Sorensen, *Phys. Rev. E* **59**, 3048 (1999).
- [9] A.C. Price, L.B. Sorensen, S.D. Kevan, J. Toner, A. Poniewierski, and R. Holyst, *Phys. Rev. Lett.* **82**, 755 (1999).
- [10] H.-Yi Chen and D. Jasnow, *Phys. Rev. E* **61**, 493 (2000).
- [11] A.N. Shalaginov and D.E. Sullivan, *Phys. Rev. E* **62**, 699 (2000).
- [12] A. Fera, I.P. Dolbnya, G. Grubel, H.G. Muller, B.I. Ostrovskii, A.N. Shalaginov, and W.H. de Jeu, *Phys. Rev. Lett.* **85**, 2316 (2000).
- [13] V.P. Romanov and S.V. Ul'yanov, *Phys. Rev. E* **63**, 031706 (2001).
- [14] V.P. Romanov and S.V. Ul'yanov, *Phys. Rev. E* **65**, 021706 (2002).
- [15] R.E. Geer, R. Shashidhar, A.F. Thibodeaux, and R.S. Duran, *Phys. Rev. Lett.* **71**, 1391 (1993).
- [16] R.E. Geer and R. Shashidhar, *Phys. Rev. E* **51**, R8 (1995).
- [17] R.E. Geer, S.B. Qadri, R. Shashidhar, A.F. Thibodeaux, and R.S. Duran, *Phys. Rev. E* **52**, 671 (1995).
- [18] D.K.G. de Boer, A.J.G. Leenaers, M.W.J. van der Weilen, M.A. Cohen Stuart, G.J. Fleer, R.P. Nieuwhof, A.T.M. Marcellis, and E.J.R. Sudholter, *Physica A* **248**, 274 (1998).
- [19] D.K.G. de Boer, *Phys. Rev. E* **59**, 1880 (1999).
- [20] T. Salditt, T.H. Metzger, J. Peisl, B. Reinker, M. Moske, and K. Samwer, *Europhys. Lett.* **32**, 331 (1995).
- [21] T. Salditt, C. Munster, J. Lu, M. Vogel, W. Fenzl, and A. Suvorov, *Phys. Rev. E* **60**, 7285 (1999).
- [22] A. Erdelyi and H. Bateman, *Higher Transcendental Functions* (McGraw-Hill, New York, 1953), Vol. 2.
- [23] *Handbook of Mathematical Functions. With Formulas, Graphs, and Mathematic Tables*, edited by M. Abramowitz and I. Stegun (U.S. GPO, Washington, D.C., 1964).
- [24] L. Brillouin and M. Parodi, *Propagation des Ondes dans les Milieux Periodiques* (Masson, Paris, 1956).
- [25] A. Caille, *C. R. Seances Acad. Sci., Ser. B* **274**, 891 (1972).
- [26] P.G. de Gennes and J. Prost, *The Physics of Liquid Crystals* (Clarendon, Oxford, 1993).
- [27] M.V. Fedoruk, *Asymptotics: Integrals and Series* (Nauka, Moscow, 1987) (in Russian).